Morphological Optimization by Rational Matching of Donor and Acceptor

Boosts the Efficiency of Alkylsilyl Fused Ring Polymer Solar Cells

Bin Huang[a], Lin Hu[b], Lie Chen*[a], Shanshan Chen[c], Ming Hu[a], Yinhua Zhou*[b], Youdi Zhang[a], Changduk Yang[c], Yiwang Chen[a]

[a]College of Chemistry/Institute of Polymers and Energy Chemistry (IPEC), Nanchang University, Nanchang 330031, (P. R. China).

[b]Wuhan National Laboratory for Optoelectronics, School of Optical and Electronic Information, Huazhong University of Science and Technology, Wuhan 430074, China.

[c]Department of Energy Engineering, School of Energy and Chemical Engineering, Perovtronics Research Center, Low Dimensional Carbon Materials Center, Ulsan National Institute of Science and Technology (UNIST), 50 UNIST-gil, Ulju-gun, Ulsan 44919, South Korea

Corresponding author. Tel.: +86 791 83968703; fax: +86 791 83969561. E-mail: chenlie@ncu.edu.cn (L. Chen),

yh_zhou@hust.edu.cn(Y. Zhou).

Author contributions: B. Huang and L. Hu contributed equally to this work.

Materials and Methods

General Information

All reactions and manipulations were operated under argon atmosphere and all the starting materials were purchased from commercial suppliers and used without further purification. Chloroform, Chlorobenzene, Ag (99.999%), MoO$_3$ (99.999%), ITIC and other materials were purchased from Alfa, Aldrich，Solarmer Materials Inc. and used without further purification. Indium-tin oxide (ITO) glass was purchased from Delta Technologies Limited, whereas PEDOT:PSS (Baytron PAl4083) was obtained from Bayer Inc. INCN-F and IDTT-CHO were purchased from SunaTechInc.

Electron and Hole mobility measurements

Hole and electron mobilities were measured using the space charge limited current (SCLC) method, with electron-only device of ITO/ZnO/ active layer (PBDS-T:ITIC for 1.2:1, w/w, PBDS-T:ITIC-F for 1.0: 1.0, w/w, for PBDS-T:ITIC-Th1 1.0: 1.0, w/w,) /Al for electron mobility measurement and the hole-only devices used a diode configuration of ITO/PEDOT:PSS/copolymers:ITIC (PBDS-T:ITIC for 1.2:1, w/w, PBDS-T:ITIC-F for 1.0: 1.0, w/w, for PBDS-T:ITIC-Th1 1.0: 1.0, w/w,)/MoO$_3$/Au by taking current-voltage curve in the range of -3-3 V. The SCLC mobilities were calculated by MOTT-Gurney equation, which is described by:

$$J = 9\varepsilon_0\varepsilon_r u V^2/8L^3$$

where J is the current density, L is the film thickness of active layer, ε_0 is the permittivity of free space (8.85×10^{-12} F m^{-1}), ε_r is the relative dielectric constant of the transport medium, u is the hole or electron mobility, V is the internal voltage in the device and $V = V_{appl}-V_r-V_{bi}$, where V_{appl} is the applied voltage to the device, V_r is the voltage drop due to contact resistance and series resistance across the electrodes, and V_{bi} is the built-in voltage due to the relative work function difference of the two electrodes.

Optical characterizations

UV-vis absorption spectra were recorded on a Perkin Elmer Lambda 750 spectrophotometer. All film samples were spin-cast on quartz slice substrates. Solution UV-Vis absorption spectra at elevated temperatures also were collected on a Perkin Elmer Lambda 750 Spectrophotometer. The temperature of the cuvette was controlled with a Perkin Elmer PTP 6+6 Peltier System, which is supplied by a Perkin Elmer PCB 1500 Water Peltier System. Before each measurement, the system was held for at least 10 min at the target temperature to reach thermal equilibrium. A cuvette with a stopper (Sigma Z600628) was used to avoid volatilization during the measurement. The

photoluminescence spectra (PL) were measured by photoluminescence spectroscopy (Hitachi F-7000) and Time-resolved photoluminescence were measured by an Edinburgh Instruments FLS920 spectrometer. Film-depth-dependent light absorption was performed according to literature procedures.[1]

Electrochemical characterizations

Cyclic voltammetry (CV) was performed by a Zahner IM6e electrochemical work station, using Ag/AgCl as the reference electrode, a Pt plate as the counter electrode, and a glassy carbon as the working electrode. Polymers were drop-cast onto the electrode from CB solutions to form thin films. 0.1 mol L^{-1} tetrabutylammonium hexafluorophosphate in anhydrous acetonitrile was used as the supporting electrolyte. The scan rate was 0.05 V s^{-1}. The E_{HOMO} and E_{LUMO} are calculated as refer to the eqs (1) and (2).

$$E_{HOMO} = -(E_{ox} + 4.4) \text{ eV} \qquad (1),$$
$$E_{LUMO} = -(E_{red} + 4.4) \text{ eV} \qquad (2).$$

GIWAXS measurement

The GIWAXS measurement was carried out at the PLS-II 6A U-SAXS beamline of the Pohang Accelerator Laboratory in Korea. The X-rays coming from the in-vacuum undulator (IVU) were monochromated (wavelength $\lambda = 1.10994$ Å) using a double crystal monochromator and focused both horizontally and vertically (450 (H) x 60 (V) um^2 in FWHM @ the sample position) using K-B type mirrors. The grazing incidence wide-angle X-ray scattering (GIWAXS) sample stage was equipped with a 7-axis motorized stage for the fine alignment of the sample, and the incidence angles of the X-ray beam were set to be 0.11°-0.13° for the neat and blend films. The GIWAXS patterns were recorded with a 2D CCD detector (Rayonix SX165) and an X-ray irradiation time within 100 s, dependent on the saturation level of the detector. Diffraction angles were calibrated using a sucrose standard (monoclinic, P21,

a=10.8631Å, b =8.7044Å, c=7.7624Å, and b=102.938Å) and the sample-to-detector distance was ~231 mm.

AFM and TEM characterizations

The specimen for AFM measurements was prepared using the same procedures those for fabricating devices but without MoO_3/Ag on top of the active layer. Transmission electron microscopy (TEM) images were taken on a JEOL-2100F transmission electron microscope and an internal charge-coupled device (CCD) camera. The specimen for TEM measurement was prepared by spin casting the blend solution on ITO/PEDOT:PSS substrate, then floating the film on a water surface, and transferring to TEM grids.

Device Fabrication and Characterizations

All the devices were manufactured with the structure of Glass/ITO/ ZnO /active layer/MoO_3/Ag. The conductive ITO substrates were sequentially cleaned with ultrasonication in acetone, detergent, water, and isopropanol. After drying the ITO substrates and treating the surface with UV ozone for 20 min, The ZnO precursor solution was prepared by dissolving 0.5 g of zinc acetate dihydrate ($Zn(CH_3COO)_2·2H_2O$, 99.9%, Alfa) and 138 ul of ethanolamine ($NH_2CH_2CH_2OH$, 99.5%, J&K) in 5 ml of 2-methoxyethanol ($CH_3OCH_2CH_2OH$, 99.8%, Alfa). The ZnO precursor was spin-coated at 4000 r.p.m. for 1 min onto the ITO surface. After being baked at 200 °C for 60 min in air, the ZnO-coated substrates were transferred into a nitrogen-filled glove box. Then the active layer was prepared by spin-casting chlorobenzene solution with a concentration of 20 mg mL^{-1} (chlorobenzene:DIO 99.5:0.5 volume ratio) solution to obtain about 100nm for PBDS-T:ITIC (1.2:1, w/w), 150nm for PBDS-T:ITIC-F (1.0: 1.0, w/w), and PBDS-T:ITIC-Th1 (1.0: 1.0, w/w,) and then the double-layer structure of MoO_3 (7 nm)/Ag (90 nm) was deposited over the

active layer by thermal evaporation under a vacuum chamber to accomplish the device fabrication. The effective area of one cell was 0.04 cm^2. The current-voltage ($J-V$) characteristics were measured by a Keithley 2400 Source Meter under simulated solar light (100 mW/cm^2, AM 1.5 G, Abet Solar Simulator Sun2000). The incident photon-to-electron conversion efficiency (IPCE) spectra were detected on an IPCE measuring system (Oriel Cornerstone 260 1/4 m monochromator equipped with Oriel 70613NS QTH lamp). All the measurements were performed at room temperature under ambient atmosphere.
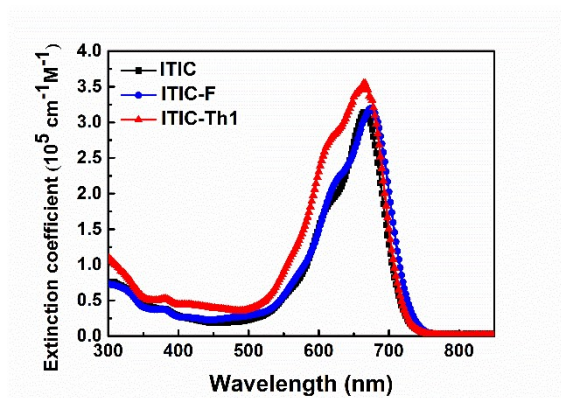
Figure S1. Absorption spectra of the ITIC, ITIC-F and ITIC-Th1 in chlorobenzene

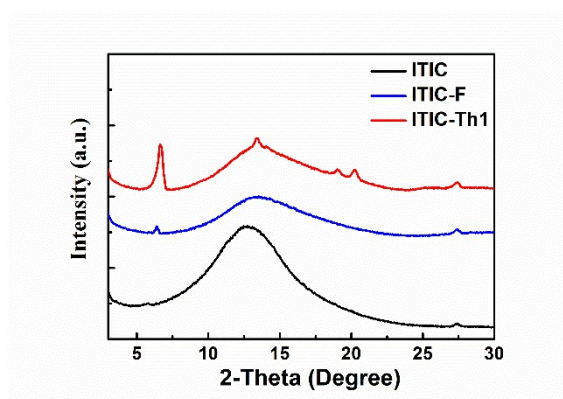solutions with concentration of 2.0×10^{-5} mol l^{-1}

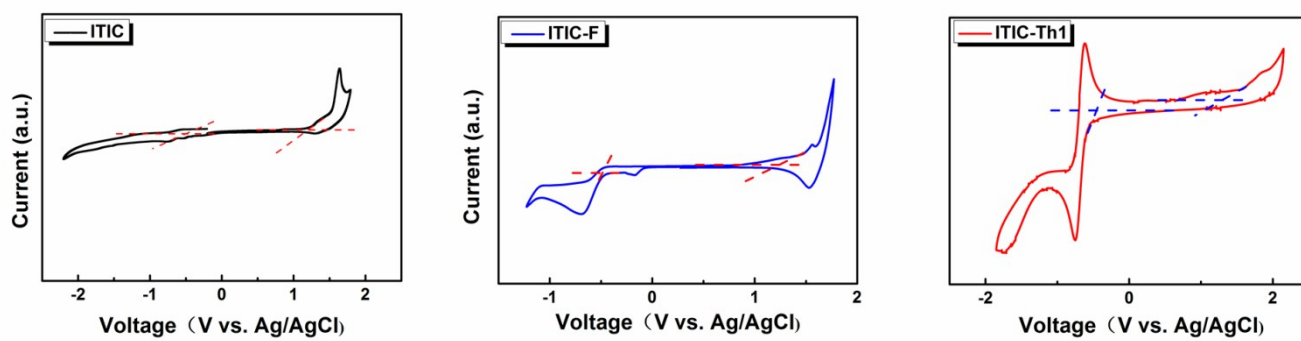**Figure S2**. XRD pattern of the molecules studied in this work.

Figure S3a.Cyclic voltammetry (CV) of the molecules thin film measured in a 0.1 M Bu$_4$NPF$_6$-CH$_3$CN solutions with a Pt electrode and an Ag/AgCl reference electrode.
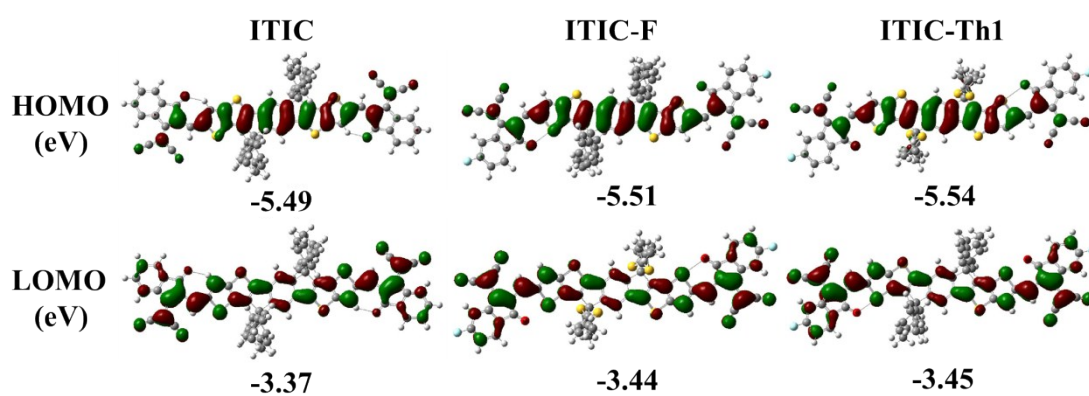

Figure S3b. Theoretical density distribution for the frontier molecular orbitals of ITIC, ITIC-F and ITIC-Th1.
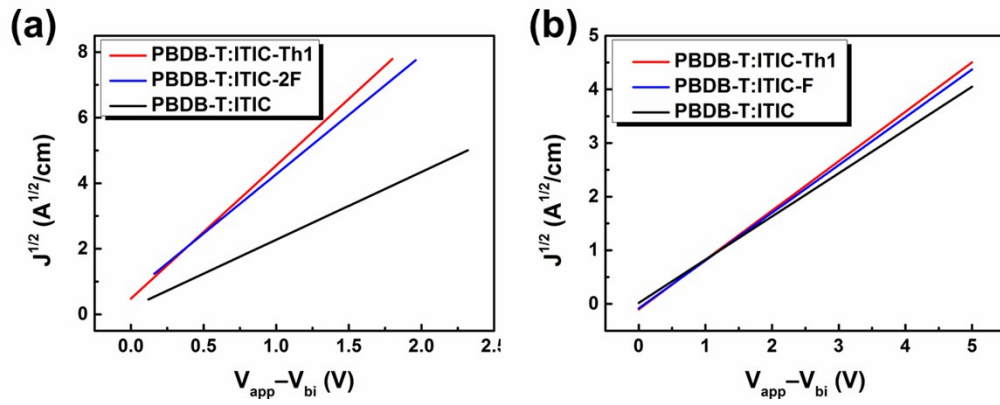
Figure S4. (a) $J^{1/2}-V$ plots of hole-only devices with active layer. (b) $J^{1/2}-V$ plots of electron-only devices with active layer.
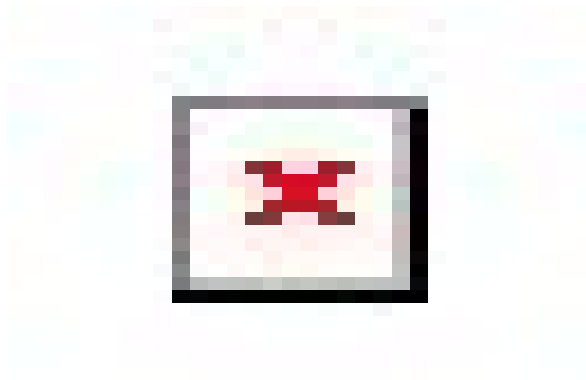
Figure S5. V_{OC} versus light intensity for PBDS-T:SMAs (ITIC, ITIC-F and ITIC-Th1)-based devices.
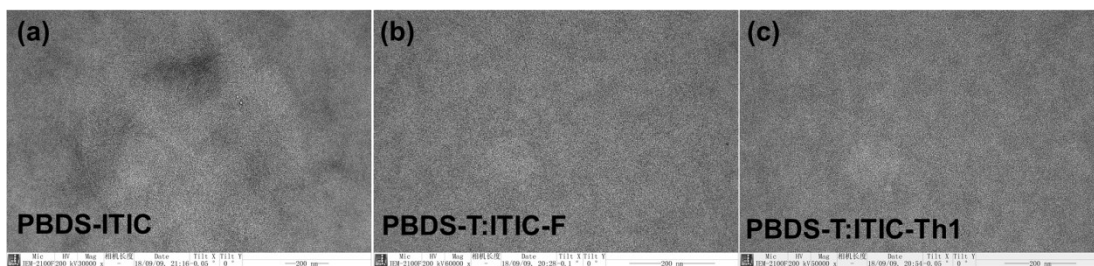
Figure S6.TEM images (a) PBDS-T:ITIC blend film; (e) PBDS-T:ITIC-F blend film and (f) PBDS-T:ITIC-Th1 blend film.

Table S1a. Photovoltaic performances of the PSCs based on PBDS-T:ITIC-Th1 with different solvent and concentration under the illumination of AM 1.5G 100 mW cm^{-2} (ITO/ZnO/active layer/MnoO$_3$/Ag)

Solvent	Concentration (mg.ml^{-1})	V_{OC} (V)	J_{SC} (cm^{-2})	FF (%)	PCE (%)
CF	12	0.90	15.7	64.5	8.5
	18	0.90	17.08	62.2	8.74
CB	20	0.87	17.08	66.1	9.83
	22	0.86	16.34	63.0	8.846

Table S1b. Photovoltaic performances of the PSCs based on PBDS-T:ITIC-Th1 with different D/A ratio under the illumination of AM 1.5G 100 mW cm^{-2} (ITO/ZnO/active layer/MnoO$_3$/Ag)

D/A ratio	V_{OC} (V)	J_{SC} (cm^{-2})	FF (%)	PCE (%)
1.5:1	0.89	16.04	62.3	8.9
1.25:1	0.89	14.86	69.4	9.2
1:1	0.87	17.87	66.4	10.3
1:1.25	0.88	16.54	64.8	9.5
1:1.5	0.90	15.68	65.3	9.2

Table S1c. Photovoltaic performances of the PSCs based on PBDS-T:ITIC-Th1 with different additive (v/v%) under the illumination of AM 1.5G 100 mW cm^{-2} (ITO/ZnO/active layer/MnoO$_3$/Ag)

Additive (v/v%)	V_{OC} (V)	J_{SC} (cm^{-2})	FF (%)	PCE (%)
0.2	0.89	18.93	69.8	11.76
0.5	0.88	19.55	70	12.04
1.0	0.87	18.67	67.2	10.88
2.0	0.87	16.74	65.9	9.57

.

Table S2. Hole and electron mobilities of the corresponding blend films.

Active layer	$\mu_h(cm^2V^{-1}s^{-1})$	$\mu_e(cm^2V^{-1}s^{-1})$	μ_h/μ_e
PBDS-T:ITIC	1.3×10^{-4}	3.6×10^{-4}	0.36
PBDS-T:ITIC-F	8.6×10^{-4}	7.5×10^{-4}	1.15
PBDS-T:ITIC-Th1	8.9×10^{-3}	9.8×10^{-3}	0.91

PL Quenching Efficiency

PL quenching efficiency was calculated according to the equation:

$$\Delta PL \quad = \quad 1 \quad - \quad \frac{PL_{blend}}{PL_{monomer}}$$

Table S3. PL quenching efficiency of the corresponding blend films.

	PBDS-T:ITIC	PBDS-T:ITIC-F	PBDB-T:ITIC-Th1
$\mathbf{\Delta PL_D}$[a)]	90%	96%	95%
$\mathbf{\Delta PL_A}$[b)]	80%	95%	91%

a) ΔPL_D is PL quenching efficiency of the blends relative to polymer donor PBDS-T;

b) ΔPL_A is PL quenching efficiency of the blends relative to SMAs (ITIC, ITIC-F and ITIC-Th1).

Table S4a. Time-resolved photoluminescence (TRPL) of BHJ at 510 nm excitation.

Blend films	τ_1 (ns)	Ratio 1(%)	τ_2 (ns)	Ratio 2(%)	τ_{ave} (ns)
PBDS-T:ITIC	0.23	89.8	2.08	10.2	0.42
PBDS-T:ITIC-F	0.27	90.5	2.43	8.5	0.45
PBDB-T:ITIC-Th1	0.37	94.3	4.44	5.7	0.60

Table S4b. Time-resolved photoluminescence (TRPL) of BHJ at 650 nm excitation.

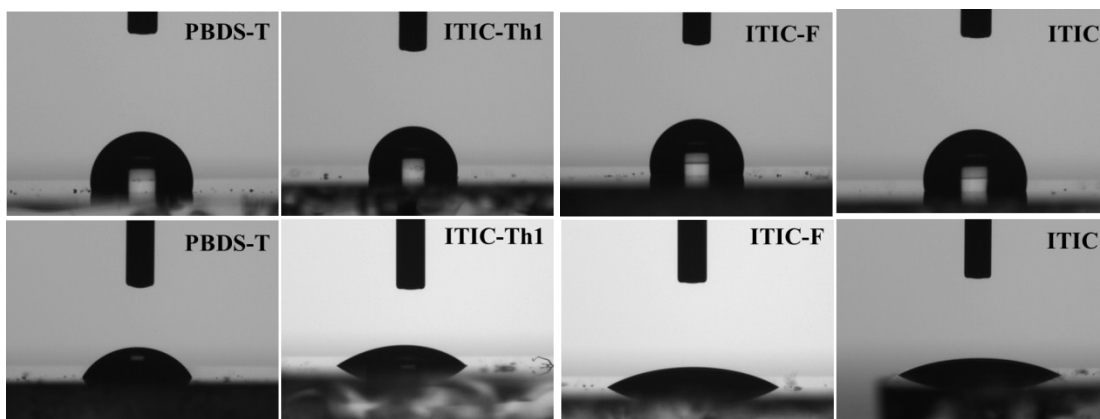| Blend films	τ_1 (ns)	Ratio 1(%)	τ_2 (ns)	Ratio 2(%)	τ_{ave} (ns)
PBDS-T:ITIC	0.23	89.8	2.08	10.2	0.42
PBDS-T:ITIC-F	0.27	90.5	2.43	8.5	0.45
PBDB-T:ITIC-Th1	0.37	94.3	4.44	5.7	0.60

Figure S8a. Views of surface contact measurements with the corresponding films. The measurements are carried out by using deionized water (upper row) and diiodomethane (under row) as the wetting liquid.
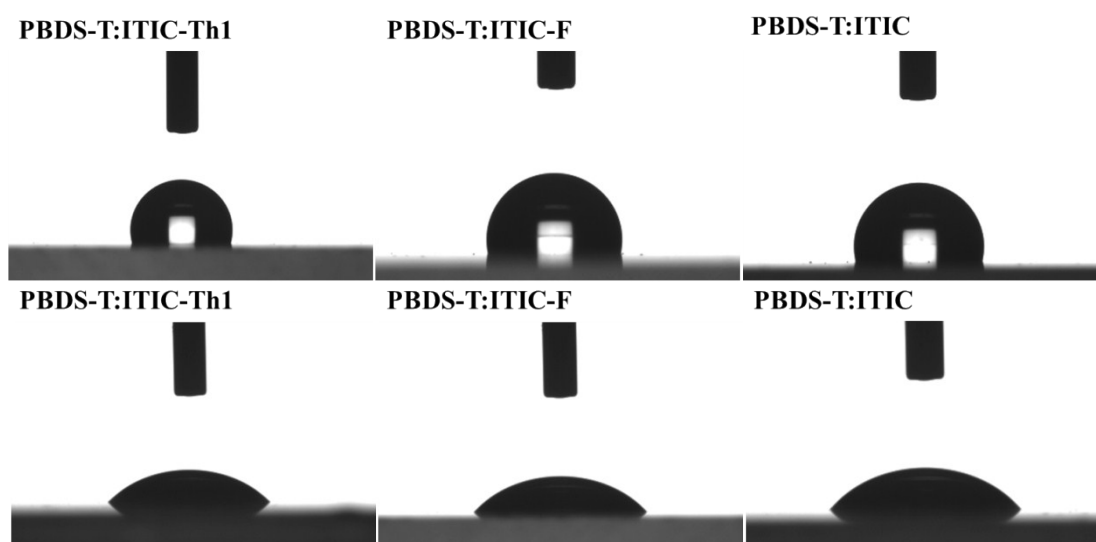

Figure S8b. Views of surface contact measurements with the blend films. The measurements are carried out by using deionized water (upper row) and diiodomethane (under row) as the wetting liquid.

Table S5a. The contact angles and surface energy parameters of the thin films.

Surface	Contac angle		γ_d [b)]	γ_p [b)]	γ
	$\theta_{water}(°)$	$\theta_{oil}(°)$[a)]	(mN m^{-1})	(mN m^{-1})	(mN m^{-1})
PBDS-T	104.21	54.45	31.76	0.03	31.79
ITIC-Th1	103.12	33.04	42.58	0.12	42.08
ITIC-F	103.46	33.76	42.60	0.13	42.72
ITIC	103.14	32.51	41.76	0.12	41.21

Table S 5b. The contact angles and surface energy parameters of the blend films.

Active layer	Contac angle	
	$\theta_{water}(°)$	$\theta_{oil}(°)$[a)]
PBDS-T:ITIC-Th1	105.00	50.47
PBDS-T:ITIC-F	104.50	48.80
PBDS-T:ITIC	105.08	50.70

[a)] θ_{oil} represents the contact angle of diiodomethane; [b)] γ_d and γ_p represent the surface free energies generated from the dispersion forces and the polar forces, respectively。